

STABILITY OF BUILT-UP CYLINDRICAL STRUCTURES WITH CONSIDERATION OF PLASTIC AND POSTBUCKLING BEHAVIOR OF THIN-WALLED COMPONENTS

G.N. Zamula, K.M. Ierusalimsky
Central Aerohydrodynamic Institute (TsAGI), Russia

Keywords: *structure, stability, buckling, nonlinear, numerical*

Abstract

Consideration is given to the challenging problem of accordance the theoretical and experimental data on stability in the case of compression and bending of stiffened shells (powerful stiffeners and thin skin) typical of fuselages of state-of-the-art transport airplanes.

Numerically obtained data were compared with results of testing the semi-full-scale cylindrical shells; in the average, the theoretical critical load is slightly higher than the critical test load. Note that not taking into account the plastic and postbuckling behavior of elements does lead to much larger discrepancy between numerical analyses and experiments.

Introduction

The problem of general instability of stiffened cylindrical shells under axial compression/bending is one of the most complicated and important problems of strength of aircraft fuselages and stiffened shells of some other aerospace vehicles. The urgency of this problem is defined by the increase of shell diameters and by the introduction of more severe requirements to structural weight saving, which result in the reduction of the relative stiffness of frames. General buckling becomes the main failure mode of such shells.

General instability, as distinct from local buckling and panel instability (shell buckling between frames) is defined here as the mode of instability characterized by the variation of frame shape and mutual displacement of frames. The problem in real statement is very complex

because of complicated geometry, loading conditions (surface curvature, non-uniformity of loads, discrete stiffening, eccentricity) and necessity of take into account such specific nonlinear features, as postbuckling skin behavior, initial imperfections, plastic deformation, etc.

Developed in [1] numerical computing method describes the mentioned above peculiarity of stiffened shells behavior, but it is in need of practical development and verification by experiment.

Improvement upon the method and comparison between computing and experimental results are carried out herein in regard to the problems of buckling of stiffened fuselages in axial compression and bending.

At the same time the computations are executed for ideal shells in bifurcation formulation using geometrically linearized, physically nonlinear theory, and a measure of unconformity (due to initial imperfections) between theoretical and experimental critical loads is evaluated by special coefficients k_c , k_b .

The results of the majority of experimental investigations published are at present of certain interest, but they can not be used for the verification of applied analytical methods. It is connected with two main reasons: (1) availability of mainly small-scale cylinders and absence of simulation of all factors, influencing the general instability of aerospace structures especially aircraft fuselages; (2) absence of precise descriptions of test object and test

procedure, which are necessary for both the analysis and understanding the results. Therefore stiffened circular semi-full-scale cylinders especially designed and manufactured for compression tests and tested in TsAGI are chosen as the main objects of investigations. The results of experiments compare with computing results using method [1].

The method of practical analysis could be, in essence, semi-empirical with the correlation of critical compressive load obtained in tests N_c to the reliably determined upper theoretical load for perfect cylinder, N^* so that $k_c = N_c / N^*$. Thus the verifiable experimentally design critical load of uniform axial compression can be determined from the relationship

$$N_c = k_c N^*, \quad (1)$$

where k_c is the empirical correlation factor. In real practice the designer should take measures to reduce the sensitivity of load-carrying structure to initial imperfections and the coefficient k_c must be as close to 1 as it is possible (it differs from that in the case of thin smooth shells).

The principal possibility to 'smear' the stiffeners and to use the structurally-orthotropic model for solution of buckling problem in compression and bending is of present interest. The general conclusion was that the grid of stiffeners should be dense and regular enough, so that within the limits of one half-wave of buckle pattern several stiffeners of each direction are located (not less than two stiffeners). Only 'smeared' stiffener model can be used to account for the premature buckling and the reduction of skin stiffness and maybe the buckling of stiffener webs [1]. The mentioned condition is verified a posteriori by using the results of buckling mode analysis. If this condition is not satisfied, it is necessary to use other models considering the discreteness of stiffening elements (stringers, frames).

Separate attention should be paid to the developed approaches, related to the cases of pure bending and combined axial compression and bending of stiffened cylinder (or nonuniform compression). Since

the tests of stiffened cylindrical shells in bending show the buckle pattern typical for axial compression in compressed zones, here the concept of reduction of bending to equivalent compression is used. This reduction uses the maximum compressive load intensity taken with appropriate correlation factor k_b , which is obtained from tests and analysis in bending conditions. This approach provides the opportunity of use all methods and results, obtained for uniform compression, to the cases of bending, and eccentric compression. Being more simple for analysis and tests, the case of uniform axial compression becomes a peculiar standard, and some theoretical and practical problems mentioned above are verified with respect to this standard.

1 Analysis of nonlinear stress-strain state and instability

Let us consider in detail the algorithm using the method [1] for stiffened shell typical of fuselages, consisted of metallic (isotropic) skin stiffened by longitudinal and transversal ribs, under axial compression and bending (Fig.1).

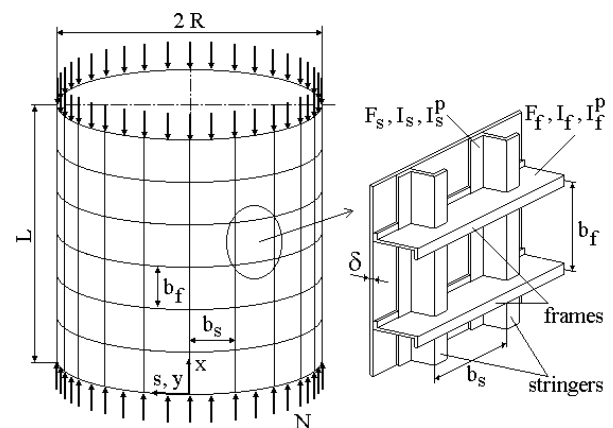


Fig.1. Stringer-and-frame-stiffened cylinder

The flow chart of the algorithm is shown in Fig.2, where the main stages are presented:

- Consecutive step-by-step increase of external loads proportionally to one load parameter $t_{k+1} = t_k + \Delta t_k$, $k = 1, 2, 3, \dots$
- Determination of momentless prebuckling stress-strain state (sss). If the plastic

deformations arise in the elements of cylinder at some particular step of load or the skin buckles, the analysis is carried out by the method of iterations to determine 'secant' material characteristics for this elements and/or secant reduction factors, considering the skin stiffness reduction in postbuckling state E^s , μ^s , φ^s . If above mentioned iteration process is converged, the 'tangent' stiffness parameters are calculated. These parameters are used in neutral balance equations.

- Analysis of bifurcation criterion and calculation of critical value of load parameter t^* .

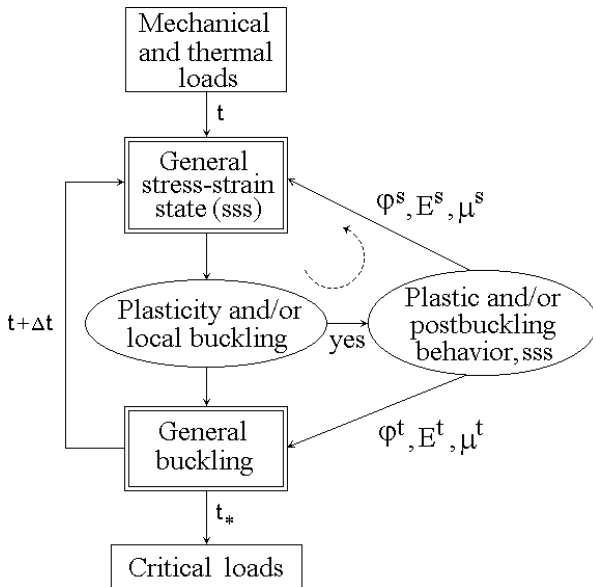


Fig.2. The scheme of stability analysis of thin-walled structure with the plastic state and/or local skin buckling

1.1 Computation of prebuckling nonlinear stress state

Prebuckling stress resultants $N_x^0 = P / (2\pi R)$ and $N_s^0 = -p R$ are related to the stresses in skin and stiffeners by the following way:

$$\begin{aligned} N_x^0 &= \sigma_s F_s / b_s + \bar{\sigma}_x^0 \delta, \\ N_s^0 &= \sigma_f F_f / b_f + \bar{\sigma}_y^0 \delta, \end{aligned} \quad (2)$$

where σ_s , σ_f = stresses in stringers and frames, respectively; $\bar{\sigma}_x^0$, $\bar{\sigma}_y^0$ = average stresses in buckled skin; F_s , F_f = areas of stringers and frames, respectively.

The deformations of stringers and frames are found from relations

$$\varepsilon_s = \sigma_s / E_s^s, \quad \varepsilon_f = \sigma_f / E_f^s, \quad (3)$$

where E_s^s , E_f^s = secant moduli of stringer and frame material under uniaxial loading in plastic range.

The skin deformations on lines of its interface with stringers and frames, respectively, are expressed in a form:

$$\begin{aligned} \varepsilon_x &= \bar{\sigma}_x^0 / E_x^s - \mu_{yx}^s \bar{\sigma}_y^0 / E_y^s, \\ \varepsilon_y &= \bar{\sigma}_y^0 / E_y^s - \mu_{xy}^s \bar{\sigma}_x^0 / E_x^s, \end{aligned} \quad (4)$$

where E_x^s , E_y^s = secant moduli of buckled skin in plastic range; μ_{xy}^s , μ_{yx}^s = secant Poisson's ratios of buckled skin in plastic range.

Using the skin-stringer (skin-frame) deformation compatibility conditions along the lines of their interface, it is possible to write down:

$$\varepsilon_x = \varepsilon_s, \quad \varepsilon_y = \varepsilon_f. \quad (5)$$

Skin stresses can be obtained from equations (4) in a form:

$$\begin{aligned} \bar{\sigma}_x^0 &= \frac{E_x^s}{1 - \mu_{xy}^s \mu_{yx}^s} (\varepsilon_x + \mu_{yx}^s \varepsilon_y), \\ \bar{\sigma}_y^0 &= \frac{E_y^s}{1 - \mu_{xy}^s \mu_{yx}^s} (\varepsilon_s + \mu_{xy}^s \varepsilon_x), \end{aligned} \quad (6)$$

substituting relations (6) into equation (2) and using relationships (3) and (5), we obtain:

$$\begin{aligned} \sigma_s &= (N_x^0 \delta_{22} - N_s^0 \delta_{12}) / \Delta, \\ \sigma_f &= (N_s^0 \delta_{11} - N_x^0 \delta_{21}) / \Delta, \end{aligned} \quad (7)$$

where

$$\Delta = \delta_{11} \delta_{22} - \delta_{12} \delta_{21}, \quad \delta_{11} = F_s / b_s + h r_{xs}^s,$$

$$\delta_{12} = \delta \mu_{yx}^s r_{xf}^s, \quad \delta_{22} = F_f / b_f + \delta r_{yf}^s,$$

$$\delta_{21} = \delta \mu_{xy}^s r_{ys}^s, \quad (8)$$

$$r_{xs}^s = \frac{\varphi_x^s E_o^s}{E_s^s (1 - \mu_{xy}^s \mu_{yx}^s)}, \quad r_{xf}^s = \frac{\varphi_x^s E_o^s}{E_f^s (1 - \mu_{xy}^s \mu_{yx}^s)},$$

$$r_{yf}^s = \frac{\varphi_y^s E_o^s}{E_f^s (1 - \mu_{xy}^s \mu_{yx}^s)}, \quad r_{ys}^s = \frac{\varphi_y^s E_o^s}{E_s^s (1 - \mu_{xy}^s \mu_{yx}^s)},$$

E_o^s = secant moduli of skin material in plastic range; φ_x^s, φ_y^s = secant reduction factors, considering the skin stiffness reduction due to its early buckling [1].

Using σ_s and σ_f obtained from equations (3) and (5), ε_s and ε_f are determined. Using equation (6), the average stress in skin $\bar{\sigma}_x^o$ and $\bar{\sigma}_y^o$ can be obtained. The real skin stresses on the lines of its interface with stringer and frame are expressed as follows:

$$\sigma_x^o = \bar{\sigma}_x^o / \varphi_x^s, \quad \sigma_y^o = \bar{\sigma}_y^o / \varphi_y^s. \quad (9)$$

The secant moduli of skin E_o^s , stringer E_s^s and frame E_f^s in equations (8) and (9) are determined by using nonlinear stress-strain state diagrams $\sigma - \varepsilon$ for appropriate materials:

$$E_o^s = \frac{\sigma_i}{\varepsilon_i + (1 - 2\mu_o) \sigma_i / E_o},$$

$$E_s^s = \sigma_s / \varepsilon_s, \quad E_f^s = \sigma_f / \varepsilon_f, \quad (10)$$

where

$$\varepsilon_i = \frac{\sqrt{2}}{3} \sqrt{(\varepsilon_x - \varepsilon_y)^2 + (\varepsilon_y - \varepsilon_z)^2 + (\varepsilon_z - \varepsilon_x)^2}$$

$$\sigma_i = \sqrt{\sigma_x^{o2} + \sigma_y^{o2} - \sigma_x^o \sigma_y^o},$$

$$\varepsilon_z = \frac{\mu_s^o}{E_o^s} (\sigma_x^o + \sigma_y^o), \quad (11)$$

Secant Poisson's ratio of buckled skin in plastic range is expressed as follows:

$$\mu_o^s = 0.5 - (0.5 - \mu_o) E_o^s / E_o, \quad (12)$$

where E_o, μ_o = elastic modulus and Poisson's ratio of skin material in elastic range.

The iteration method is used for determination of nonlinear prebuckling state on each load step.

At the first iteration, it is assumed that $E_o^s = E_o, \mu_o^s = \mu_o, E_s^s = E_s, E_f^s = E_f$ and $\varphi_x^s = \varphi_y^s = 1$. The stresses σ_s and σ_f are found from equations (7), deformations $\varepsilon_s = \varepsilon_x, \varepsilon_f = \varepsilon_y$ are found from equations (2), skin stress is found from equations (6). The intensities of deformation and skin stress are found from equations (11); denominator in the first equation (10) $\varepsilon_i^r = \varepsilon_i + (1 - 2\mu_o) \sigma_i / E_o$ is found by taking into account equation (12).

The E_o^s, E_s^s, E_f^s are determined for obtained deformations $\varepsilon_s, \varepsilon_f$ and ε_i^r by using nonlinear stress-strain diagrams $\sigma - \varepsilon$ for appropriate materials. New secant reduction factors are found by using equations from [1]. The iterative process converges quickly; it is completed, when the variables attain the required accuracy $\approx 10^{-3}$.

1.2 Calculation of tangent stiffness parameters and buckling load

After computing the nonlinear prebuckling stress state on each load step, the variable tangent stiffness parameters of cylinder are calculated.

Considering that the equations for instability analysis in [1] are written in terms of small increments of prebuckling (initial) state of equilibrium parameters, the stiffness parameters in these equations are calculated at variations of nonlinear stiffness parameters of initial state. In this connection, the tangent moduli of stiffened cylinder elements and tangent reduction factors enter into the expressions for stiffness parameters:

$$B_{11}^t = E_s^t (r_{ts} \delta + F_s / b_s),$$

$$B_{22}^t = E_f^t (r_{tf} \delta + F_f / b_f),$$

$$\begin{aligned}
 B_{12}^t &= B_{21}^t = \frac{\mu_{yx}^t E_x^t \delta}{1 - \mu_{yx}^t \mu_{xy}^t}, \\
 B_{33}^t &= G_{xy}^t h + G_{sf}^t h_{sf}, \quad (13) \\
 D_{11}^t &= E_s^t \left[r_{ts} \left(\delta^3 / 12 + \delta h_1^2 \right) + I_s / b_s + \right. \\
 &\quad \left. + F_s / b_s (z_s - h_1)^2 \right], \\
 D_{22}^t &= E_f^t \left[r_{tf} \left(\delta^3 / 12 + \delta h_2^2 \right) + \right. \\
 &\quad \left. + I_f / b_f + F_f / b_f (z_f - h_2)^2 \right], \\
 D_{12}^t &= D_{21}^t = \mu_{yx}^t \frac{E_x^t \delta^3}{12(1 - \mu_{yx}^t \mu_{xy}^t)}, \\
 D_{33}^t &= G_{xy}^t \frac{\delta^3}{6} + \frac{G_s^t I_s^p}{2b_s} + \frac{G_f^t I_f^p}{2b_f},
 \end{aligned}$$

where:

$$r_{ts} = \frac{E_x^t}{E_s^t (1 - \mu_{yx}^t \mu_{xy}^t)}, \quad r_{tf} = \frac{E_y^t}{E_f^t (1 - \mu_{yx}^t \mu_{xy}^t)},$$

$E_x^t, E_y^t, E_s^t, E_f^t$ = tangent moduli of materials of skin, stringer and frame at achieved stress level, respectively [1];

μ_{xy}^t, μ_{yx}^t = tangent Poisson's ratios for skin buckled in plastic range [1];

G_s^t, G_f^t = tangent shear moduli of materials of stringer and frame, respectively;

$F_s, F_f, I_s, I_f, I_s^p, I_f^p$ = areas, own moments of inertia and torsion constants for stringer and frame, respectively;

z_s, z_f = distances from centroids of stringer/frame cross-section to the skin midsurface, respectively;

h_1, h_2 = distances from centroids of stringer/frame cross-section with adjoined effective skin to the skin midsurface, respectively.

Critical loads are calculated in accordance with [1] using tangent stiffness parameters (13).

The empirical rule can be used to check in the applicability of 'stiffener smearing'

procedure and the quality of analysis by using orthotropic model: if length of half-waves of buckle pattern in longitudinal and circumference directions $\ell_x \geq 1.5 b_f$ and $\ell_s \geq 1.5 b_s$, than the results of general instability analysis are considered to be satisfactory. If the mentioned inequalities are not satisfied, the analysis can not be considered to be satisfactory. In this case, the method is required, which takes into account the discrete frame arrangement.

The analysis of cylinder buckling between frames (panel form) is also conducted by using the above mentioned algorithm. It is assumed, that the number of half-waves of lengthwise buckle pattern m is equal to the number of spans between frames ($\ell_x = b_f$) and that the frames are located in nodal lines. In this connection, their areas F_f and moments of inertia I_f do not contribute to the calculation of

stiffness parameters B_{22}^t and D_{22}^t .

The analysis of instability of stiffened cylinder requires to perform two analyses:

- analysis of general instability,
- analysis of buckling between frames.

The least load from two obtained ones should be taken as the determining load.

2 Calculations and buckling analysis for the case of axial compression

To illustrate the influence of plasticity and skin local buckling upon general buckling let us consider calculation results for stiffened shell with parameters typical of fuselages of state-of-the-art airplanes. Fig.3 shows the shell, its sizes and stiffener parameters. The diagram shows schematically values of critical compression load obtained by calculations: 1 – without taking into account plasticity and local buckling, 2 – with taking into account plasticity and without taking into account local buckling, 3 – with taking into account local buckling and without taking into account plasticity, 4 – with taking into account plasticity and local buckling. Comparison of these values shows influence of each nonlinear effect on

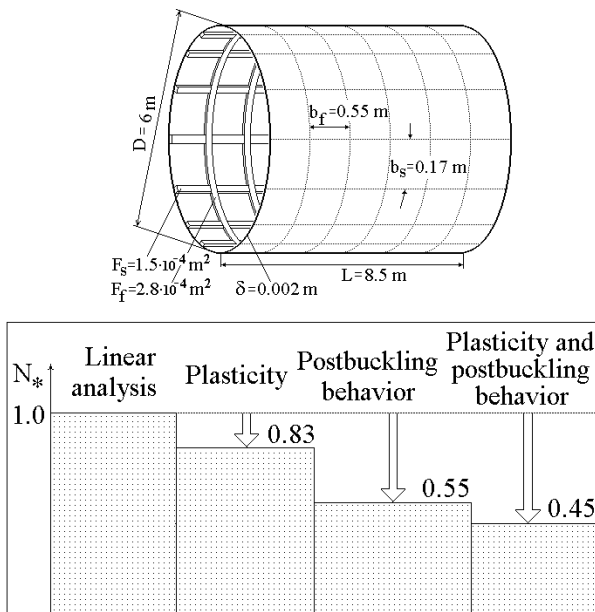


Fig.3. General buckling loads considering nonlinear effects

calculated critical load. Summary influence of both the linearity for parameters considered is very considerable (>50%) in comparison with the linear result.

The analysis of convergence of theoretical and experimental results was carried out concerning to buckling of full-scale cylinders tested in TsAGI in axial compression. The riveted cylinders are typical of fuselages in all essential details. Sizes and relative stiffness characteristics of the cylinders are close to the parameters of fuselages. The circular cylinders have diameter 1500 mm, skin thickness $\delta=1$ mm. Skin and stiffeners are made of aluminium alloy. The cylinders have different length, different number and shape of longitudinal and transversal stiffeners. According to parameters combination the cylinders are subdivided to 19 types. From 1 to 3 cylinders of every type was manufactured, 41 cylinders in all. Comparison of theoretical and experimental results is shown in Fig.4.

The mean value of relationship $k_c^m=0.9$ was obtained for total group of cylinders. This value shows that the theoretical values of buckling load N_* (using method [1]) is greater than the test values N_c by $\approx 10\%$ on the average. Statistical analysis of all cylinders as

single group shows distribution of k_c close to the normal distribution with mean square deviation $=0.099$ and with coefficient of variation $= 11\%$. Fig.4 shows also comparison of tests results and calculation results using the same method but without taking into account

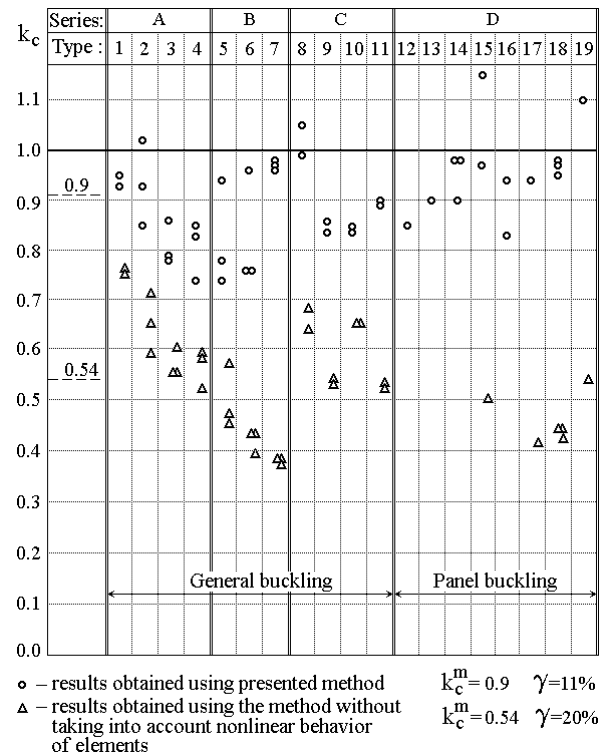


Fig.4. Correlation factor $k_c = N_c / N_*$

plasticity and skin local buckling. In this case the mean value $k_c=0.54$ and coefficient of variation $\approx 20\%$ were obtained. These results shows importance of taking into account nonlinear effects above mentioned for analysis of real aircraft stiffened shells.

3 Buckling in bending

The following method is used for analysis of general instability of stiffened cylinders in pure bending.

If more than three half-waves ℓ_s of buckling pattern of uniform axial compression of this cylinder are contained in a compressed zone of cross section of bent cylinder, then

$$N_{I*} = N_*, \tag{14}$$

STABILITY OF BUILT-UP CYLINDRICAL STRUCTURES WITH CONSIDERATION OF PLASTIC AND POSTBUCKLING BEHAVIOR OF THIN-WALLED COMPONENTS

where N_{I*} = amplitude of stress resultant, arising in compressed zone due to pure bending, N_* = stress resultant at buckling in uniform axial compression, calculated by the method [2].

If less than three half-waves l_s of buckling pattern of uniform axial compression of this cylinder are contained in a compressed zone of cross section of bent cylinder, then N_{I*} is calculated by using equations from [1] where number of half-waves in circumference direction is set to 3.

The buckling analysis for cylinders subjected to combined bending and compression uses the same method.

To demonstrate of accuracy of proposed method, the refined buckling analysis was conducted for one of tested cylinder named B.2 in eccentric compression by using numerical method of stress-strain state and buckling analysis [1], [2], which enables to take into account the variation of load and stiffness parameters in circumference of the cylinder under bending. Stiffness parameters are calculated in the some points set in circumference. The number of these points should be sufficient for satisfactory description of functions $B_{ij}^t = B_{ij}^t(s)$, $D_{ij}^t = D_{ij}^t(s)$ ($i, j = 1,2,3$). The results of refined calculation of buckling loads P and M for cylinder B.2 in combined bending and compression are listed in Table 1.

Table 1

P, kN	M, kNm	N_{I*} , kN/m
2160	0	465.1
1531	258.5	470.0
1076	456.6	471.6
542	689	472.8
0	915	472.5

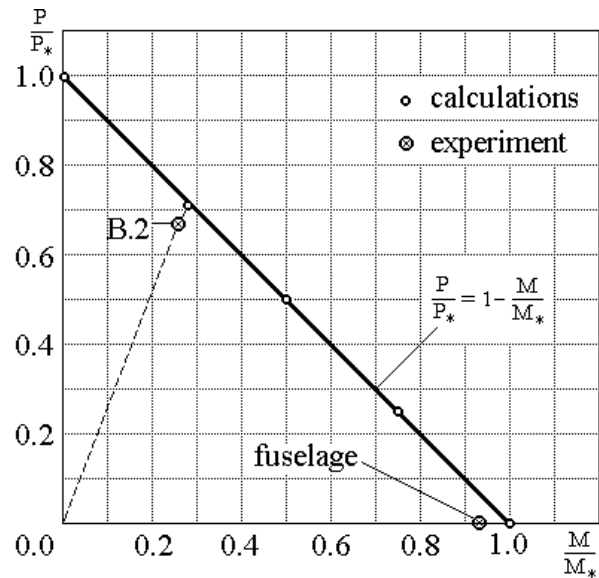


Fig.5. Stability boundary for cylinder under combined compression and bending

The data are plotted in Fig.5 against relative coordinate system P / P_* , M / M_* . The theoretical points fit well to the straight line $P / P_* + M / M_* = 1$, which is shown in Fig.5. The amplitude value of compressive stress resultant at buckling N_{I*} remains practically constant (see N_{I*} in Table 1). The difference between buckling load of pure axial compression $N_* = 465.1$ kN/m and the amplitude value of compressive stress resultant at buckling in pure bending $N_{I*} = 472.5$ kN/m does not exceed 2%.

Fig.5 shows the result obtained in test of cylinder B.2 under combined compression and bending. Fig.6 shows the buckle pattern of cylinder B.2 obtained numerically in pure compression, compression with bending and in pure bending.

After completion of static tests program of one passenger aircraft, special failure tests were conducted on this structure in order to study general instability behavior of its fuselage in bending. Test loads corresponded to one of the landing cases.

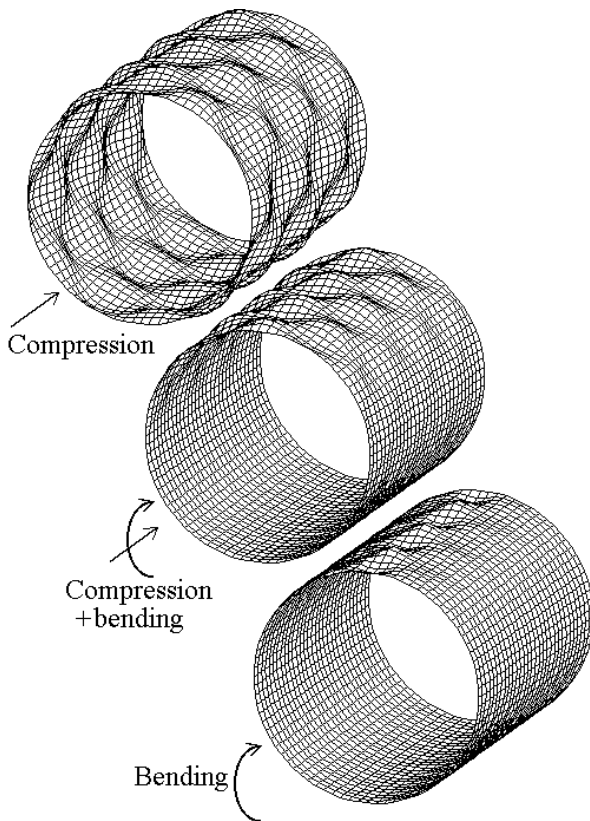


Fig.6. Buckle patterns (cylinder B.2)

These loads resulted in symmetrical down-bending of fuselage. Maximum value of bending moment was realized in regular zone of fuselage located behind the center wing box, which is schematically shown in Fig.7. The distribution of stress resultant (along contour) is shown in the same Fig.

The loading of aircraft was conducted by whiffle-tree system by steps of 10% of ultimate load M^P up to 70% of M^P . After that, the structure was loaded continuously up to failure. In each step, detailed strain gage measurements of stress state were carried out. In final stage of test, high-speed filming of the bottom fuselage in zone of expected buckling was conducted.

During the tests, fuselage failure occurred at bending moment $M_b = 1.38 \cdot M^P$.

For determination of amplitude of load intensity N_b in bottom area of fuselage corresponding to the failure, the analysis of nonlinear stress state of fuselage section in bending was conducted. The nonlinearity arises

during loading due to non-uniform skin stiffness reduction along the contour and probable occurrence of plastic deformations, depending on the achieved level of stress in fuselage elements. The model for stress analysis was designed taking into account real skin thickness, stringer arrangement and their areas.

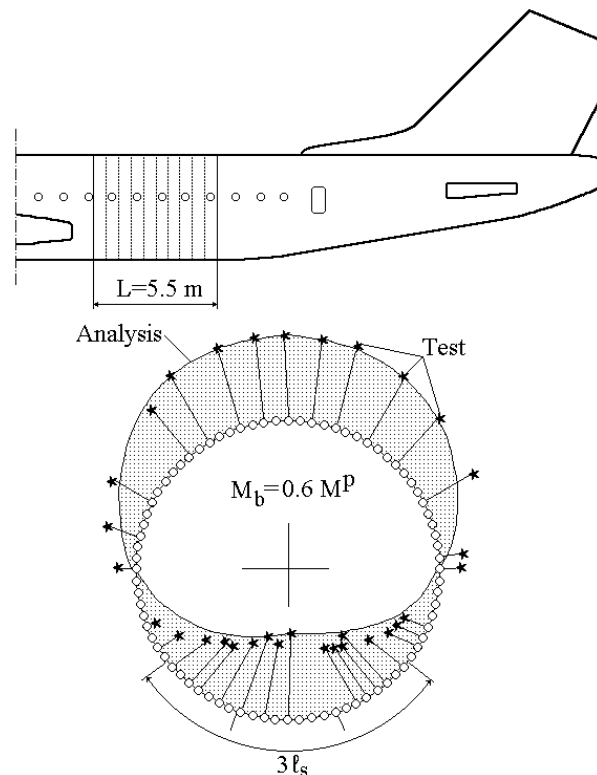


Fig.7. Model of full-scale fuselage

The results of stress analysis for various values of M_b are shown on Fig.8, where the dependence of N_b on M_b is shown. N_b values were calculated by using stresses in stringers and in skin, and reduction factors. The dependencies of the part of load which is carried by stringers N_s , and part loads carried by skin N_o , on bending moment M_b . Here $N_b = N_s + N_o$. The amplitude value of load per unit length N_b in bottom area of fuselage in prebuckling state under bending moment $M_b = 1.38 \cdot M^P$ corresponding to buckling is $N_b = 1500$ kN/m.

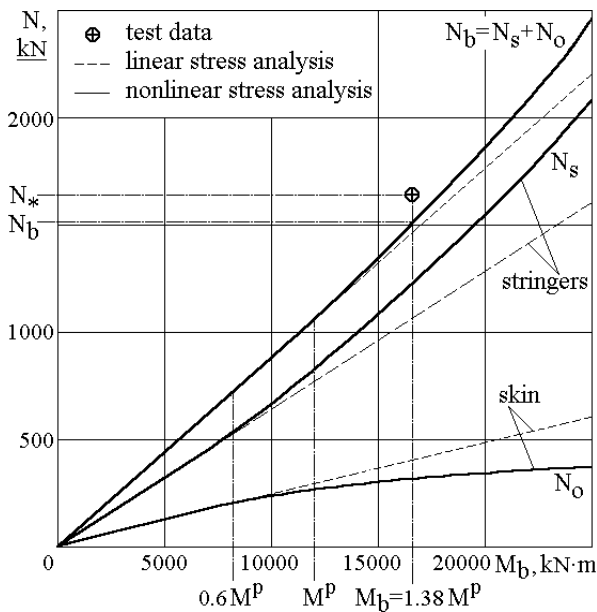


Fig.8. Depending of amplitude value of compression stress resultant on bending moment of full-scale fuselage

Further the analysis of buckling of fuselage section in compression was executed. It was considered, that the cylinder has the regular structure, the same as the structure of bottom fuselage panel. As a result of analysis the following is obtained:

$$N^* = 1647 \text{ kN/m}; \quad m^* = 6, \quad n^* = 5;$$

$$\ell_x = 0.92 \text{ m}, \quad \ell_s = 1.32 \text{ m}.$$

It was determined, that in compressed zone more than three half-wave lengths of buckling pattern are located. In accordance with the rule stated above, $N_{I^*} = N^*$.

Comparing N_b with N^* , we establish that

$$k_b = N_b / N^* = 0.91.$$

Consequently, the analysis predicts the real critical value of N_b in bending and eccentric compression well, when using the same correlation factor $k_b \cong k_c^m$ ($N_b = k_b N^*$) as in pure compression.

Conclusion

The obtained results of tests and analyses are compared for the problem of general buckling of stiffened shells of aircraft fuselages.

The results of analyses using the method [1] and tests, value of correlation factor $k_c^m = 0.9$, scatter of test data (coefficient of variation = 11%) show a good agreement.

Further improvement of the method of fuselage general instability analysis in axial compression is scarcely possible at present time, because of deficiency of test data and presence of many uncontrollable parameters like shape imperfections, eccentricities, residual stresses, etc. In case of bending, the method which uses the replacement of bending by equivalent compression (and taking into account pressure, torsion, etc.) requires further development and refinement.

Reference

- [1] Zamula G N, Ierusalimsky K M. Stability and elements postbuckling behavior of complex composite structure. *Proc. of 20th ICAS Congress*, Sorrento, Italy, September 8-13, 1996.
- [2] Zamula G N. Numerical analysis of thin-walled structure with a buckled skin. *WCCM-II*, Stuttgart, Germany, August 27-31, 1990.